Coupling between the Atmospheric Circulation and the Ocean Wave Field: An Idealized Case

PIERO LIONELLO

Department of Physics, University of Padua, Padua, Italy

P. MALGUZZI AND A. BUZZI

FISBAT-CNR, Bologna, Italy

(Manuscript received 5 February 1996, in final form 25 October 1996)

ABSTRACT

This work studies the two-way coupling between the atmospheric circulation and the ocean surface wave field, as it is described by the recent observations and theories on the dependence of the sea surface roughness on the ocean wave spectrum. The effect of the coupling on the atmospheric variables and the ocean wave field is analyzed by implementing both the atmospheric and the ocean wave models in a periodic channel and simulating a wide range of different situations. In a strong atmospheric cyclone, in comparison to the one-way coupling, the two-way coupling attenuates the depth of the pressure minimum and significantly reduces the wave height and surface wind speed while it increases the momentum flux. The heat and moisture fluxes are increased if they are computed using the same wave-dependent roughness that is used for the momentum flux, while they are decreased if they are computed using the Charnock relation. The effects are proportionally larger for extreme storms because the time required for the deepening of the low pressure is much shorter than the time required by the windsea to reach a well-developed state.

1. Introduction: The two-way coupling between the atmosphere and the ocean wave field

This numerical study analyzes the evolution of a low pressure system over the sea and of the resulting oceanic wave field in the presence of a two-way coupling between the atmospheric and ocean wave models. Usually, it is assumed that there is a one-way coupling between the atmosphere and the surface waves without any feedback from the ocean waves generated by the surface wind on the atmospheric circulation. According to recent research results, the surface stress is a function not only of the wind velocity and atmospheric stability, but also of the wave spectrum. Consequently, there is a two-way coupling between the atmosphere and waves that influences the stress over the sea surface.

Ocean waves play an important role in the transfer of momentum across the air–sea interface because the downward flux of momentum from the atmosphere τ_a consists of two contributions, $\tau_a = \tau_{aw} + \tau_{ao}$, representing the flux from the atmosphere to the waves and the ocean current, respectively. The value of the ratio τ_{aw}/τ_a, on which there is no general agreement, depends on the stage of wave development. Certainly τ_{aw} is not negligible and a reasonable estimate is $0.15\tau_a \leq \tau_{aw} \leq \tau_a$. However, the wave field retains only a small part of τ_{aw}, and the momentum is almost completely transferred to the underlying upper ocean because the wave amplitude is limited by breaking that determines a flux τ_{wo} from the waves to the current. Consequently, the net momentum flux to the wave field, $\tau_w = \partial M_w/\partial t = \tau_{aw} - \tau_{wo}$, resulting in wave growth, is typically a few percent of τ_a (Lionello et al. 1993). Therefore, since the momentum transfer from the atmosphere to the ocean current is not direct, the surface ocean waves play a fundamental role in the transfer of momentum across the air–sea interface, even though the momentum ends up almost completely in ocean currents.

The crucial role of the waves at the air–sea interface explains why they have to be taken into account in the description of the atmospheric boundary layer over the ocean. The effect of the waves is generally described by the Charnock relation (Charnock 1955)

$$z_0 = \alpha_C \frac{\tau_a}{\rho_a g}, \tag{1}$$

where α_C is a dimensionless constant, g is the acceleration of gravity, and ρ_a is the air density. Equation (1) implicitly assumes that z_0, the sea surface roughness, is not constant but is proportional to the swh (significant

Corresponding author address: Dr. Piero Lionello, Department of Physics, University of Padua, via Marzolo 8, 35131 Padua, Italy.
E-mail: piero@borexo.pd.infn.it

wave height) of the fully developed windsea, which scales as $\tau_a/\rho_a g$ (Kitaigorodsky 1973). Recent studies on the momentum flux over the sea suggest that, at fixed wind speed, the roughness reaches a maximum when the windsea is young (initial stage) and decreases during its subsequent development (Donelan 1982; Geernaert et al. 1987; Janssen 1989; Janssen et al. 1989; Smith et al. 1992). It follows that Charnock's relation has to be modified in order to reproduce the variation of the sea surface roughness during the windsea development. So far, no similar dependence of heat flux on wave spectrum has been suggested by observations or theoretical studies.

When an atmospheric low pressure system develops over the ocean, the associated surface wind generates ocean waves. If the wind were blowing in a steady direction and with constant speed, the waves would become progressively higher, longer, and less steep. In this situation the waves would progressively get older and the sea surface roughness would decrease. However, the pattern of the surface wind during the development of a storm is complex. The wind changes continuously in direction and intensity, both in time and space; it continuously generates new young waves and stops acting on old waves travelling out of the storm. The surface roughness is larger than the value predicted by Charnock's relation in the regions where the waves are young, while it is lower in the region where the waves are old. The effect of such variations on marine storms is investigated in this study.

Specifically, numerical models of atmospheric circulation and surface wave field are used in order to estimate the magnitude of the effect of the wave-dependent surface stress on both the atmospheric variables and the wave field. The results of two-way coupled and one-way coupled models, based on Charnock's relation, are compared. In the presence of rapidly varying wind fields, the continuous generation of young waves is expected, at first approximation, to enhance the surface stress, decreasing the intensity of the atmospheric low pressure system. The surface wind speed is therefore diminished due to both the increase in surface roughness and the reduction in pressure gradient. Consequently the wave field intensity is also reduced. Thus, the overall effect of the two-way coupling will be the damping of both the atmospheric and wave fields.

The quantitative evaluation of the effect is carried out by analyzing the growth of an atmospheric baroclinic instability in a periodic channel simulating the development of a midlatitude cyclone. A similar idealized case has been studied (Doyle 1994) in which the mesoscale and synoptic-scale structure of the atmospheric low pressure system were found to be significantly modified by the variation of the sea surface roughness, whereas a global simulation with two-way coupled models (Weber et al. 1993) found no significant effect of the waves on the atmospheric patterns. These contradictory conclusions are reanalyzed in this study, and the factors conditioning the effect are identified by exploring the sensitivity of the results to the intensity of the cyclone, its wavelength, the presence of coastlines, horizontal resolution of the models, and air–sea temperature difference. The intensity of the developing depression was varied by modifying the initial meridional profile of temperature and zonal wavelength of the instability. Simple coastlines splitting the channel into subbasins have been introduced in order to decrease the age of the windsea by reducing the fetch. The grid step was changed in order to explore the influence of resolution on the coupling mechanisms. Finally, since there is no precise indication of an effect of the ocean waves on heat fluxes, the coupling was restricted to momentum flux.

The paper is organized in the following way. Section 2 reviews the present understanding of the coupling mechanism. Section 3 briefly presents the models used in this study and describes how they are coupled. Section 4 describes the characteristics of the evolution of the two-way coupled system with reference to a simulated case of intense cyclogenesis. Section 5 analyzes the different simulations in order to assess the magnitude of the effect of the wave field on the coupled atmosphere–wave system. Section 6 summarizes the findings of the study.

2. The dependence of the surface stress on the ocean wave spectrum

The dependence of the surface stress on the ocean wave field has been extensively investigated over the last few years. This section provides a very brief review of the available experimental evidence and theoretical understanding.

Both experiments and theoretical models summarize their results by expressing the sea surface roughness z_0 (or the drag coefficient C_D or the friction velocity u_*) as a function of a single parameter called wave age, defined as $\alpha_{10} = C_p/u_{10}$, where u_{10} is the 10-m wind speed and C_p is the phase speed of the spectral peak frequency. The wave age indicates the stage of wave development because the phase speed C_p increases progressively during wave growth. Sometimes the definition $\alpha_* = C_p/u_*$ is preferred (Geernaert et al. 1987; Janssen 1989; Smith et al. 1992).[1] This simple parameterization of z_0 is adequate in an idealized situation where wave growth is limited either by time or fetch, wind is steady, and therefore the wave spectrum can be parameterized. Models including dependence on the wind direction and the wave spectrum are needed for the modeling of realistic situations.

[1] Note that if the surface stress is influenced by ocean waves, the ratio u_*/u_{10} depends on wave age and wind speed.

a. Experimental evidence

Four different datasets were used to investigate the dependence of the sea surface roughness on the ocean wave field. They are denoted as follows.

- NSP: Measurements acquited at the North Sea Platform located in the German Bight (Geernaert et al. 1987). The surface stress and u_{10} were measured, the peak frequency was estimated from the wind speed and the fetch using an empirical relation.
- BSlab: A dataset consisting of measurements carried out in Bass Strait and a collection of published, including laboratory, data (Toba et al. 1990). In Bass Strait the one-dimensional spectrum and the wind speed u_{10} were measured, while the surface stress was estimated from the wave height and period using an empirical relation.
- HEXOS: Measurements collected on a Dutch platform in the North Sea during the Humidity Exchange Over the Sea Experiment (Smith et al. 1992). Measurements included the surface stress, the one-dimensional wave spectrum, and u_{10}.
- LO: Measurements collected on a research platform in Lake Ontario (Donelan 1982; Donelan et al. 1993). Measurements included the surface stress, the one-dimensional wave spectrum, and u_{10}.

Two datasets, HEXOS and LO, indicate that the sea surface roughness decreases as the wave age increases. The NSP observations are consistent with this finding, although in this experiment wave age was estimated from wind speed and fetch, and it is not clear whether this has conditioned the results (Geernaert et al. 1987). The BSlab dataset suggested the opposite conclusion. This inconsistency can be explained (Donelan et al. 1993) because 1) laboratory data are not representative of open field situations, 2) BS measurements were carried out in shallow water, and 3) stress was indirectly estimated from wave height and period using an empirical relation. Therefore, the conclusions of Toba et al. do not apply in general to open field measurements. The parameterization based on the HEXOS and LO data are in good agreement. The HEXOS data were used by Smith et al. (1992), who proposed the parameterization

$$\alpha_C = \frac{0.48}{\alpha_*}. \tag{2}$$

Donelan used both LO and HEXOS datasets to produce a different fit:

$$z_0 = 6.7 \times 10^{-4} \sigma \alpha_{10}^{2.6}, \tag{3}$$

where σ is the rms wave height. This is approximately equivalent to Eq. (2) because σ scales with U^2/g.

In conclusion, the available experimental results support a dependence of the surface roughness on wave age. A quantitative estimate can be immediately derived from Eq. (2). During wave development, α_* varies approximately from 10 (young waves) to 30 (old waves), producing a factor of 3 reduction of the Charnock constant and an approximate variation of C_D of 40% for a 25 m s^{-1} wind and 20% for a 5 m s^{-1} wind.

b. Models of the sea surface roughness

On the theoretical side there are two possible explanations for the dependence of the sea surface roughness on the sea state and they have both been used in models capable of reproducing the observed data.

The first explanation is based on the effect of waves on atmospheric turbulence when the flow is aerodynamically rough and the airflow detaches from the sea surface on the wave crests. In fact, there is experimental evidence that the short waves break on the crests of long waves and that surface stress undergoes a large increase in correspondence with wave breaking because of the produced detachment of airflow from the sea surface (Banner and Melville 1976). The roughness elements of the sea surface can therefore be assumed proportional to the height of high-frequency waves of phase speed greater than u_* (Melville 1977). During the development of the wave spectrum, the energy contained in the high-frequency range decreases[2] (Hasselmann et al. 1973). Moreover the short waves are advected by the long wave orbital motion. Therefore, the speed of the roughness elements on the crests of long waves increases as the spectrum grows and, correspondingly, their effectiveness to produce airflow detachment decreases. Both mechanisms produce the decrease of z_0 with wave age. A similar view has been adopted by Donelan (1982) in his model of the sea surface roughness.

The second explanation is based on the wave-induced stress associated with wave-coherent fluctuation in the airflow, which implies an effect of the waves on the wind profile (Janssen 1989; Janssen et al. 1989; Makin et al. 1995). Both studies resolved the structure of the constant stress boundary layer where $\partial\tau_a/\partial z = 0$, with the condition $\tau_a = \tau_{aw} + \tau_\nu + \tau_t$. The overall stress results from the superposition of turbulent stress τ_t, viscous stress τ_ν, and wave-induced stress τ_{aw}, which is specified on the basis of previous studies by the authors. It was assumed that the Miles resonance mechanism determined the wave growth. Both studies show a large τ_{aw} near the sea surface, while at a higher level turbulence support the entire stress and the profile is logarithmic. Therefore, the effect of waves results in a wave-dependent effective roughness. Janssen obtains

$$z_0 = \frac{\hat{\alpha}_C \tau_a}{\rho_a g \sqrt{1 - \tau_{aw}/\tau_a}}, \tag{4}$$

[2] There are experimental indications of a large variation of the tail level, but results depend on the frequency range analyzed and on the power law used to fit the spectral level. Consequently, the variation of the tail level is at present controversial.

where $\hat{\alpha}_C = 0.01$ is a ''reduced'' Charnock's constant. Makin obtains

$$z_0 = \frac{0.14\nu}{\sqrt{\tau_a - \tau_{aw}}}. \quad (5)$$

If a large variation in the short wave energy during the development of the wave spectrum, and a consequently large variation of τ_{aw} is prescribed (Janssen 1989; Janssen et al. 1989), the numerical simulations of the time-limited wave growth give results that are in agreement with Eqs. (2) and (3). Both Janssen's theory and Donelan's fit determine a similar decrease of C_D and z_0 during the wave growth. When the sea is young ($\alpha_{10} = 0.5$) they are approximately equivalent to the choice $\alpha_C = 0.032$, which has already been used to reproduce the increase of the sea roughness due to the waves (Mastenbroek et al. 1993). When the sea is old ($\alpha_{10} \approx 1.0$), they imply a larger roughness than the choice ($\alpha_C = 0.0185$, which was found to be the best fit to a large set of available data representing the average over different wave age values (Wu 1982). Janssen's model is consequently capable of reproducing the observed data and is suitable for this study.[3]

3. The models

This study involves three models that are incorporated in a single code that couples them: the BOLAM atmospheric circulation model (Bologna Limited Area Model; Buzzi et al. 1994), the ocean wave model WAM (The WAMDI Group 1988), and a model of the sea surface roughness (Janssen 1991) that determines the dynamics of the coupling.

The BOLAM model is a gridpoint, hydrostatic model in sigma coordinates, computing zonal and meridional wind components (u, v), potential temperature θ, specific humidity h, and surface pressure p_s. The physics of the model includes parameterization of vertical diffusion in the planetary boundary layer depending on the Richardson number, dry adiabatic adjustment, soil water and energy balance (the sea surface temperature is prescribed), radiation, cloud effects, large-scale precipitation, condensation, evaporation, and moist convection. A fourth-order horizontal diffusion is added to the prognostic equations except in the tendency of surface pressure p_s, while second-order horizontal diffusion is applied to the divergence of the horizontal velocity. Vertical discretization is of the Lorentz type (vertical velocity is defined at intermediate levels between the levels of the prognostic variables) with a variable step that gives higher resolution near the surface. Horizontal discretization adopts the Arakawa C-grid. Time integration is leapfrog, with an implicit treatment of the terms describing gravity wave propagation and Asselin filter to suppress time splitting. Horizontal diffusion terms are integrated with a forward scheme over two model time steps.

The WAM wave model solves the energy transfer equation for the wave spectrum. The equation describes the variation of the wave spectrum F in space and time due to the advection of energy and local interactions. The wave spectrum is locally modified by the input of energy from the wind, the redistribution of energy due to nonlinear interactions and energy dissipation due to wave breaking. These processes are represented by the source functions S_{in}, S_{nl}, and S_{ds} respectively. The energy propagation and the integration of the source function are treated numerically using different techniques. The advective term is integrated with a first-order upwind scheme. The source function is integrated with an implicit scheme that allows an integration time step greater than the dynamic adjustment time of the highest frequencies in the model prognostic range. The wave spectrum is discretized using 12 directions and 25 frequencies extending from 0.041 to 0.42 Hz with a logarithmic increment $f_{n+1} = 1.1 f_n$. The prognostic region where the energy transfer equation is explicitly solved is limited to frequencies less than $f_{nf} = \max(2.5\overline{f}, 4f_{\text{PM}})$, where f_{PM} is the Pierson–Moskowitz frequency and $\overline{f}$ is the mean frequency. Beyond f_{nf} the spectrum is extended by continuity with an f^{-5} tail, which is necessary to compute the nonlinear interactions and the mean quantities occurring in the dissipation source function.

A model of the surface roughness and stress has been included in the WAM code (Hasselmann et al. 1993) in order to replace Charnock's relation with a model of the feedback of the ocean wave field on the neutral atmospheric boundary layer (Janssen 1991). This model describes the effect of the wave on surface stress while avoiding the computation of the boundary layer vertical structure, which would be too expensive for numerical weather and wave prediction. The wave contribution τ_{aw} to the total stress τ_a is computed from the wind input source function S_{in}, which is based on an analytical approximation of the results obtained with the quasi-linear theory of wave generation. Given the wind speed at 10 m u_{10} and the wave-induced stress τ_{aw}, the total stress and the surface roughness are determined from an iterative solution of

$$\tau_a = C_D u_{10}^2, \quad (6)$$

$$C_D = \left(\frac{k}{\log[10/z_0]}\right)^2, \quad (7)$$

and Eq. (4).

In the numerical experiments described in this study the atmospheric circulation model BOLAM and the ocean wave model WAM are run in parallel. Each model has its own time step. In the WAM model the advection

[3] The model of Makin et al. could also reproduce the observed data, but the authors did not assume a large variation of τ_{aw}.

term is integrated with an explicit scheme and the CFL stability criterion requires a propagation time step Δt_W:

$$\Delta t_W < \frac{\Delta s_{\min}}{C_{g\max}} = \frac{4\pi f_1 \Delta s_{\min}}{g}, \tag{8}$$

where $\Delta s_{\min}$ is the minimum grid step, $C_{g\max}$ is the maximum group speed, and f_1 is the lowest frequency in the model range. The BOLAM model adopts a semi-implicit scheme that permits the use of an integration step Δt_B larger than the limit imposed by the CFL criterion for the linear propagation of atmospheric gravity waves. Hence, Δt_B is limited only by advection. Coupling takes place every $\Delta t_C = N_B \Delta t_B = N_W \Delta t_W$. In the low-resolution experiment of this study $\Delta t_C = 20$ min, $\Delta t_W = 10$ min, $\Delta t_B = 4$ min; that is, coupling takes place every two time steps of WAM and five time steps of BOLAM. In the high-resolution experiment $\Delta t_C = 10$ min, $\Delta t_W = 10$ min, $\Delta t_B = 1$ min; that is, coupling takes place every time step of WAM and ten time steps of BOLAM.

This scheme has the advantage of providing the ocean wave model with wind fields of high time resolution that would not be available as standard output of the atmospheric circulation model. In this implementation a new wind field is accessed by WAM every 20 min, while normally the output of BOLAM would be archived to disk every 3 or 6 h. Therefore, the time resolution of the ocean wave model is increased.

The model framework allows both one-way and two-way coupling. When the one-way coupling scheme is used, the atmospheric model computes the surface wind or the stress that forces the ocean wave model, but there is no feedback from the ocean wave model to the atmospheric circulation model. In the one-way coupling scheme BOLAM computes the 10 m wind speed u_{10} that is required by WAM. The Charnock formula is used in the computation of the 10-m wind speed u_{10} and surface stress. The surface stress τ is given as $\tau = \tau_N F(z_N, \text{Ri}, z_0)$, where τ_N is the neutral stress computed using Charnock relation (1) with $\alpha_C = 0.0185$, and F a function of the Richardson number Ri, the sea surface roughness z_0, and the lowest atmospheric model level z_N. The function F accounts for the effect of the air–sea temperature difference on the momentum flux (Louis et al. 1981). In the two-way coupling scheme the computation of τ_N is carried out using Eqs. (4), (6), and (7), and the roughness given by Eq. (4) is used in the computation of u_{10}. Since there is no clear evidence of an effect of the wave field on the heat and moisture fluxes, the code allows them to be computed using the Charnock formula or, alternatively, the wave-dependent roughness. The dependence of the model results depending on the type of coupling is explored in this study.

4. The effect of the wave field on intense cyclogenesis

In this section we consider an idealized case of intense marine cyclogenesis in order to describe the effect of the two-way coupling on the atmospheric and ocean fields. Both the atmospheric and the ocean wave model have been implemented in a periodic channel on the sphere extending in latitude from 16° to 71°N. The channel length (longitudinal extension) is 43.5°.

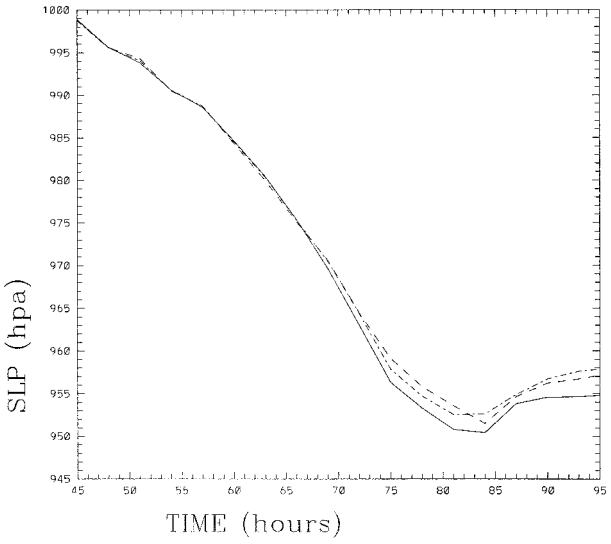

FIG. 1. Minimum SLP (sea level pressure in hPa) as function of time (in hours from the beginning of the simulation denoted with ○s in Table 1 and Figs. 11–14. The continuous line represents the one-way coupled experiment. The dashed line represents the two-way coupled experiment. The dashed–dotted line represents the two-way coupled experiment, but with the heat flux computed using the Charnock relation.

The initial state has been chosen to represent rather realistic midlatitude winter conditions, including a troposphere and a stratosphere having meridional temperature gradients of opposite sign with maximum intensity at the midlatitude of the channel. A westerly jet, in thermal wind equilibrium with the temperature field, reaches its maximum speed at the tropopause, near the channel center, and vanishes at the surface. Relatively high values of relative humidity (about 95%) are prescribed in the troposphere at middle and high latitudes, gradually decreasing toward the southern boundary and toward the tropopause. The SST kept fixed during each run, is zonally uniform and is prescribed to be equal to the initial value of the air temperature of the lowest model level. A small geostrophic perturbation of geopotential and wind, with a zonal wavelength corresponding to the channel length, is superimposed on the zonal initial state. Because of the imposed north–south temperature gradient, the initial state is baroclinically unstable. The presence of a substantial amount of moisture leading to a release of latent heat in the atmosphere enhances this instability (see, e.g., Emanuel et al. 1987), leading to a rapid growth of the perturbation. In fact, we simulate a strong oceanic cyclogenesis, which ends up with a deep cyclone and an associated ocean wave field.

Figure 1 shows the evolution of the pressure minimum for the case denoted with "○"s in Table 1. The

TABLE 1. List of the simulations discussed in this paper, notation used for plotting them in Figs. 1–4, and a short description of their characteristics.

	List of the simulations				
RUN	Model resolution (deg)	Channel length (deg)	North–South SST difference (°C)	Min SLP (hPa)	Characteristic features
●w	1.5 × 1.1	49.5	28	991.8	
●m	1.5 × 1.1	49.5	36	981.1	
●s	1.5 × 1.1	49.5	42	968.8	
●e	1.5 × 1.1	49.5	48	957.8	
⊙s	1.5 × 1.1	42.5	42	968.1	
◊w	1.5 × 1.1	28.5	28	990.0	Short channel
◊m	1.5 × 1.1	28.5	36	986.4	Short channel
□m	1.5 × 1.1	28.5	36	989.5	Short channel with strips of land
□s	1.5 × 1.1	42	42	978.4	Channel with strips of land
⊕s	1.5 × 1.1	42	42	966.8	Reduced horizontal diffusion
△s	1.5 × 1.1	49.5	44	958.1	SST uniformly increased by 2°C
△e	1.5 × 1.1	49.5	48	950.1	SST uniformly increased by 2°C
▽e	1.5 × 1.1	49.5	42	975.2	SST uniformly decreased by 2°C
▽s	1.5 × 1.1	49.5	52	959.5	SST uniformly decreased by 2°C
○vw	0.75 × 0.55	43.5	26	988.1	
○s	0.75 × 0.55	43.5	42	951.5	
○wS	0.75 × 0.55	28.5	28	984.6	Short channel
○sM	0.75 × 0.55	43.5	42	951.5	Heat and moisture fluxes based on Charnock
○sD	0.75 × 0.55	43.5	42	950.0	No precipitation (dry cyclone)

one-way coupled case reaches a minimum value of 950.4 hPa. The difference between the one-way (continuous line) and the two-way coupled (dashed line) experiments becomes visible only during the second half of the deepening phase of the cyclone, when the intense surface wind produces a young windsea and, consequently, a high value of the sea surface roughness. The increased friction diminishes the intensity of the cyclone (the maximum reduction of the pressure minimum is 2.8 hPa). Both the development time and the average eastward propagation speed of the pressure minimum (approximately 14 m s^{-1}) are not changed by the two-way coupling.

Figure 2 shows the slp (sea level pressure) pattern after 84 hours from the beginning of the simulation. Panel (a) shows the SLP in the simulation with one-way coupling and panel (b) shows the difference between one-way and two-way coupling (positive difference indicates that the values are higher in the two-way coupled simulation). The structure of the cyclone is similar in the two experiments. The two-way coupled case is less intense, with differences restricted to the central core of the storm.

The action of the coupling can be understood by considering the wave age distribution shown in Fig. 3. In the storm area the age is less than 0.6 and a higher roughness is expected, except in the cyclone core where the wave age is large, because the wind is low and high waves, previously generated, are present. In the storm area, the two-way coupling gives a roughness approximately three times larger, becoming five times larger ahead of the pressure minimum. On the contrary, the area where the wave age is larger than 1.0 units (shaded in Fig. 3) is associated with the presence of a swell radiated all around the cyclone with a diminished roughness by approximately a factor of 5. Figure 3 shows that the pattern of the wave age is not symmetric around the center of the storm. Ahead of the pressure minimum, where a strong wind (associated with a prefrontal low-level jet) starts blowing over the old waves left from the previous passage of the storm, the waves are younger than behind it. Consequently, the effect of the two-way coupling on the air–sea fluxes is most intense and systematic in the northern and eastern sections of the cyclone.

The increased roughness in the central part of the storm resulted in a generally diminished u_{10} and swh over the entire area of the storm. The reduction is significant, reaching a maximum of 20% northwest of the pressure minimum, in the region where the waves have been produced by the attenuated wind field in the northern section of the cyclone (Fig. 4).

The effect of the two-way coupling on the friction velocity does not have a constant sign over the central part of the cyclone. The friction pattern in the one-way coupled experiment shows a maximum ahead and a maximum behind the pressure minimum. In the two-way coupled experiment the maximum ahead is increased by 15% and the maximum behind is moved to the north, while the friction in the region that it formerly occupied is reduced (Fig. 5).

The asymmetric distribution of the wave age implies that the downward heat flux is percentwise more affected than the upward one by the two-way coupling. In fact, the downward heat flux is located ahead of the low pressure center in a region where the windsea is extremely young. The intensity of the upward heat flux, whose maximum is located to the southwest of the pres-

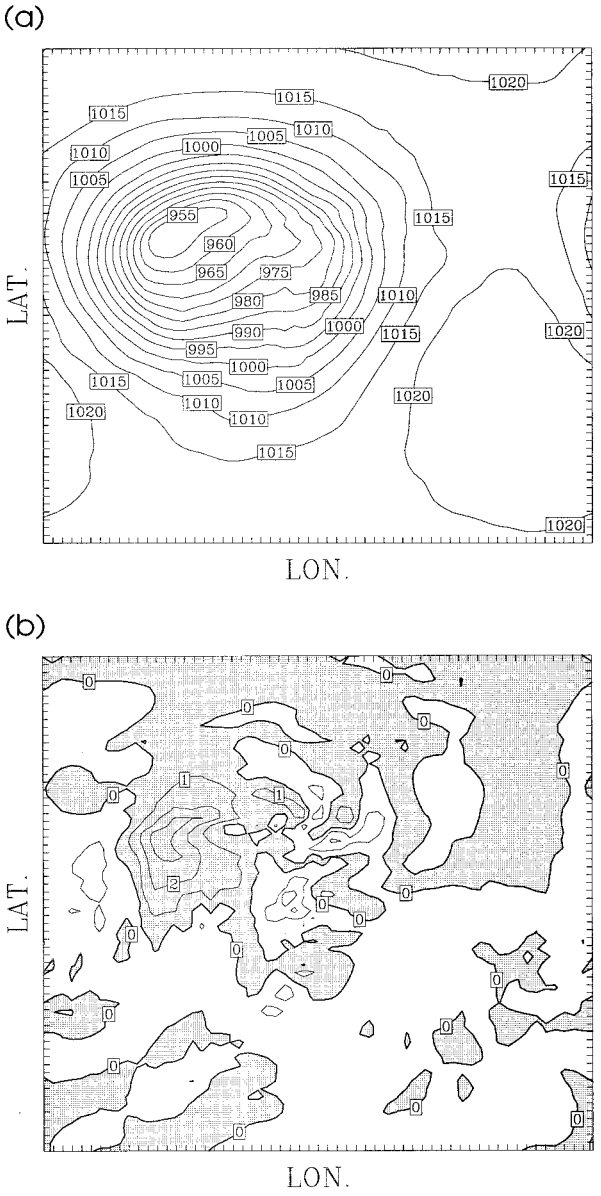

FIG. 2. Sea level pressure field at the peak of the storm, 84 hours after the beginning of the simulation denoted with ○s in Table 1 and Figs. 11–14. The central part of the channel from 25° to 60°N is shown. (a) One-way coupled experiment; the contour interval is 5 Hpa. (b) Difference between one-way and two-way coupled experiments. Positive values (shaded area) indicates the area where the two-way coupled experiment is higher; the contour line interval is 1 Hpa.

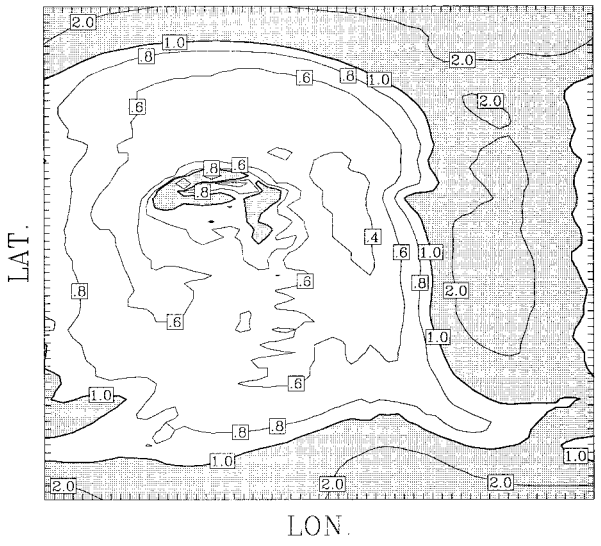

FIG. 3. Wave age field at the peak of storm in the two-way coupled experiment. The central part of the channel from 25° to 60°N is shown. The contour levels 0.4, 0.6, 0.8, 1.0, and 2.0 are shown. The dashed area denotes values of the wave age larger than 1.

sure low and in a region where all experiments give comparable values of the sea surface roughness, is not greatly modified by the two-way coupling. The differences in the latter quantity are mostly due to a shift in the position of the peak value (Fig. 6).

While the values of the surface fields have been changed by the two-way coupling, no significant effect is observed on the inner atmospheric variables. The geopotential at various pressure levels (here not shown) indicates that the diminished intensity in the two-way coupled experiment is due to a small, essentially barotropic, change in the structure of the cyclone. Particularly indicative is that the precipitation pattern, a quantity usually highly unpredictable and very sensitive to changes in the atmospheric model parameters, is only marginally affected by the coupling and the consequent variations of the heat flux. The effect of the two-way coupling on the development of the cyclone is small because on short timescales its evolution is strongly dependent on the initial unstable atmospheric condition (including the initial distribution of temperature and water vapor). On this relatively short timescale, the air–sea fluxes of momentum and heat (the quantities modified by the two-way coupling) are certainly not the main energy source for the development of the low pressure system, though they clearly influence it.

It is interesting to analyze how much the effect of two-way coupling depends on the changes directly induced by the wave field on the heat transfer coefficient. In fact, the dependence of the surface heat flux on wave age is probably not realistic because it has not been determined by measurements nor supported by theoretical studies. The case denoted with ''○s'' in Table 1 was simulated using the wave-dependent roughness in the computation of the momentum flux and Charnock formula in the computation of the heat flux; that is, the momentum flux was computed as in the two-way coupled model and the heat flux as in the one-way coupled model. The time development of the pressure minimum is shown by the dashed–dotted line in Fig. 1. The diminished intensity of the cyclone is confirmed in this experiment and, consequently, it is mainly due to the changes in the momentum transfer coefficient produced

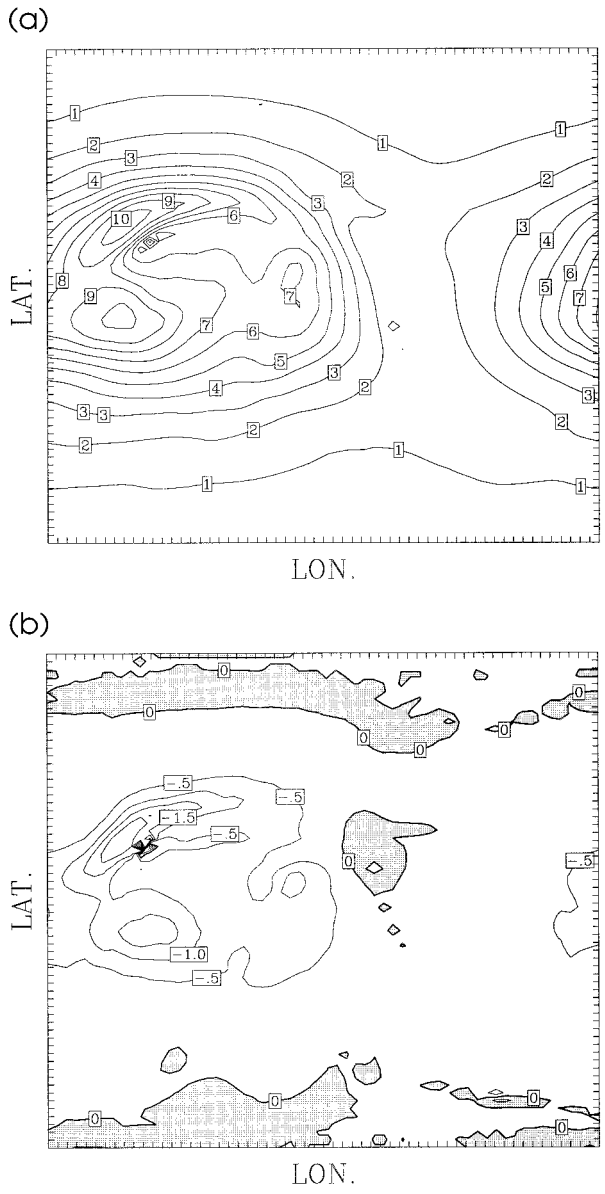

FIG. 4. The swh field at the peak of storm in the central part of the channel. (a) One-way coupled experiment; the contour interval is 1 m. (b) Difference between one-way and two-way coupled experiments. Positive values (shaded area) indicate the area where the two-way coupled experiment is higher; the contour line interval is 0.5 m.

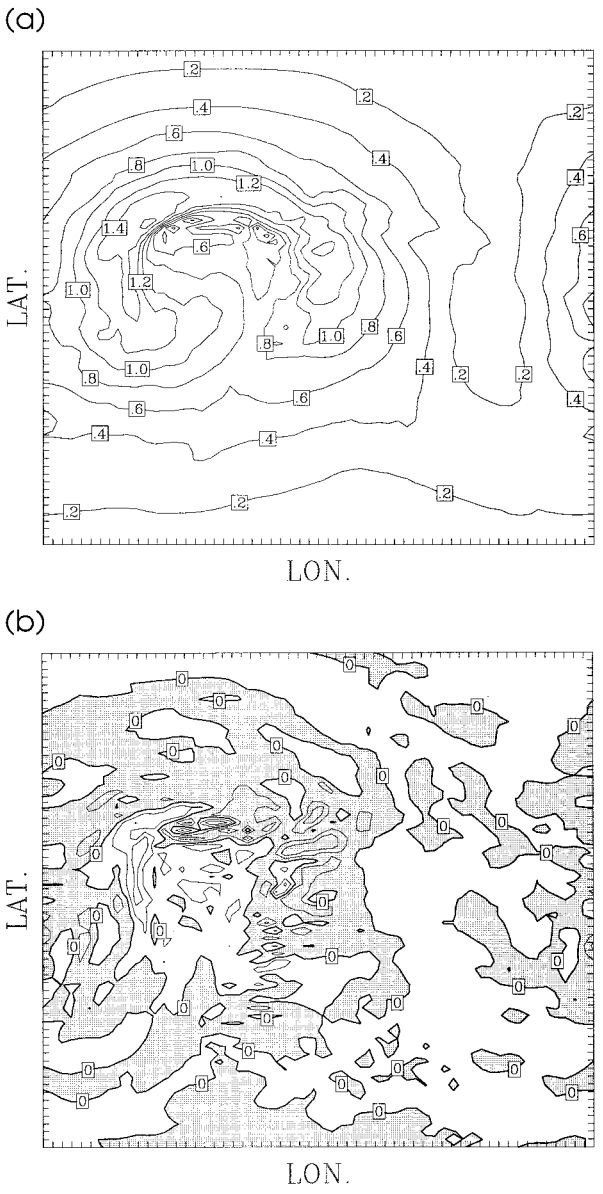

FIG. 5. The friction velocity field at the peak of storm. (a) One-way coupled experiment; The contour interval is 0.2 m s^{-1}. (b) Difference between one-way and two-way coupled experiments. Positive values (shaded area) indicate the area where the two-way coupled experiment is higher; the contour line interval is 0.1 m s^{-1}.

by the effect of the wave field on the wind profile. No appreciable change in the friction velocity, swh, and u_{10} fields was found compared to the previous two-way coupled run. The heat flux field turned out to be similar to the field of the one-way coupled experiment, though with lower intensity. In fact, since the increased friction reduced the lowest-level wind speed, the heat flux was computed using a lower roughness, and its intensity has therefore been diminished (approximately 10% for the maximum values).

The average effect throughout the development of the storm is small on surface roughness and friction velocity, while it is of some relevance to the heat flux and has a clear impact on the swh. Figures 7–10 show the temporal and zonal averages in for roughness, swh, friction velocity, and heat flux, respectively. The time average considered the fields between 58 and 99 h from the beginning of the simulation, when the main deepening of the atmospheric low pressure takes place. In the central part of the channel the temporal and zonal averages result in an average over a wide range of wave ages, while at low and high latitudes the average is

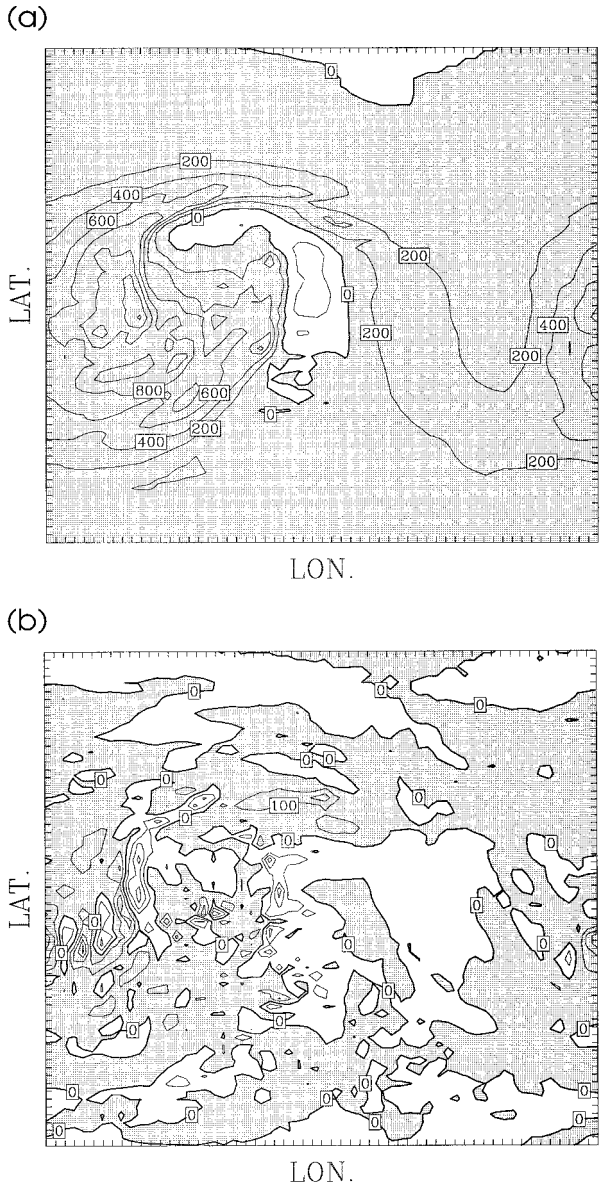

FIG. 6. The heat flux field at the peak of storm. (a) One-way coupled experiment; the shaded area indicates positive (upward) flux. The contour interval is 200 W m^{-2}. (b) Difference between the one-way and two-way coupled experiments. Positive values (shaded area) indicate the area where the two-way coupled experiment is higher; the contour line interval is 100 W m^{-2}.

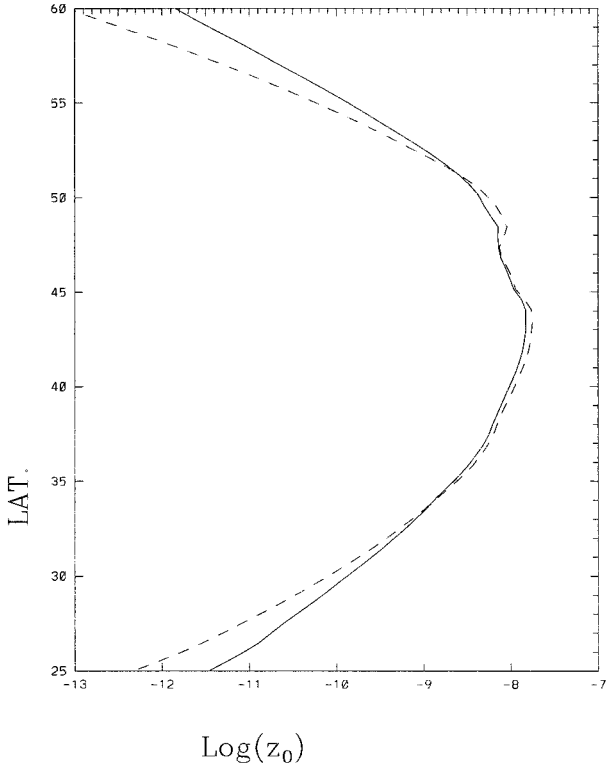

FIG. 7. Average of the natural logarithm of the sea surface roughness (in meters) as function of latitude during the evolution of the cyclone (the average has been obtained using the values from 58 to 99 h after the beginning of the simulation). The continuous line represents one-way coupled experiment. The dashed line represents the two-way coupled experiment.

biased toward old sea states. The effect of the two-way coupling is large on the average swh, which is reduced by 0.5 m in the center of the channel (Fig. 8). Figures 7 and 9 show that the Charnock relation with $\alpha_C = 0.0185$ can actually be considered representative of a mean over the various stages of the wave field development, giving average results equivalent to the two-way coupled models, as far as the sea surface roughness and momentum flux are concerned. The average heat flux (Fig. 10) may be affected in opposite ways: Compared to the one-way coupled experiment, the wave age dependent heat transfer coefficient produces a larger flux, and Charnock relation (experiment ○sM) a lower flux. The variations are approximately 10 W m^{-2}, corresponding to 5%. If the heat flux were used for forcing a model of the oceanic mixed layer, approximately a 5% variation in its deepening rate would be produced.

5. Factors that condition the effect of the two-way coupling

The evolutions of the storm according to the two-way coupled and one-way coupled models have been compared in a series of experiments with different characteristics. The purpose is to determine which quantities are affected by the two-way coupling, the size of its effect, and the factors that influence it.

The experiments are summarized in Table 1, where resolution, zonal length of the channel, overall meridional SST difference across the channel, minimum pressure in the one-way coupled experiment, and specific characteristics of each experiment are reported. In all of the experiments the models have been implemented in a periodic channel on a sphere extending in latitude from 16° to 71°N. Different channel lengths (longitudinal extensions) have been used in order to describe

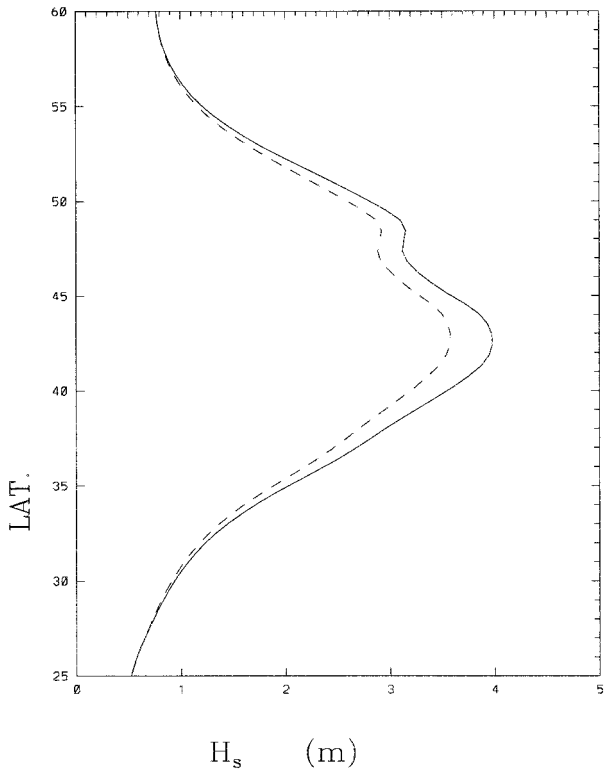

FIG. 8. As in Fig. 7 but for the average significant wave height as function of latitude. Values in meters.

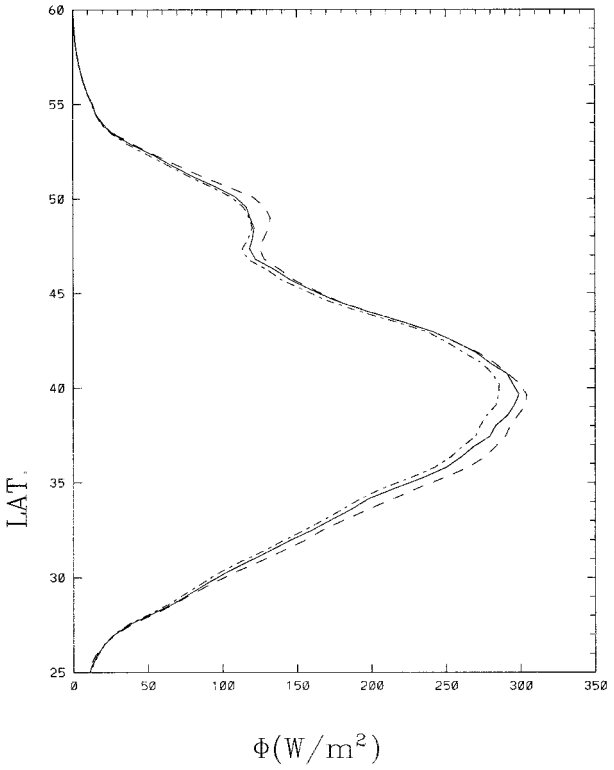

FIG. 10. As in Fig. 7 but for the average heat flux as function of latitude. Values in watts per square met. The dashed–dotted line represents two-way coupled experiment where the heat flux has been computed using Charnock relation.

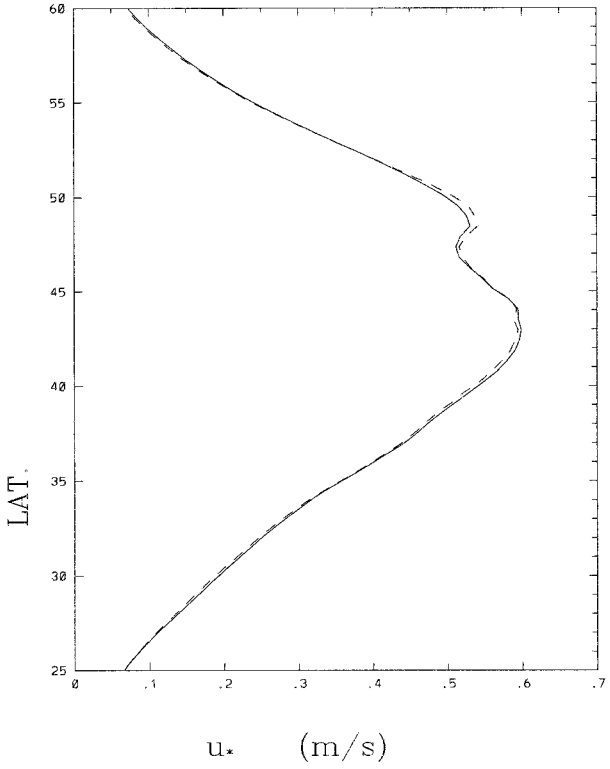

FIG. 9. As in Fig. 7 but for the average friction velocity as function of latitude. Values in meters per second.

different maximum wavelengths of the baroclinic development. In the low-resolution experiment both the atmospheric circulation and the ocean wave models have been implemented with a grid step of 1.1° lat and 1.5° long, obtaining in this way comparable zonal and meridional resolution in the center of the channel. The first subset of experiments, with a channel length of 49.5°, is denoted with a solid circle. The characters ''w'' (weak), ''m'' (medium), ''s'' (strong), and ''e'' (extreme) are added in order to indicate the increasing value of the SST temperature meridional gradient, and the consequent growth rate and final intensity of the atmospheric cyclone. The ''s'' case has been repeated with a reduced channel length (dotted circle) and the ''w'' and ''m'' cases with an even shorter channel (diamonds). The squares denote two experiments where the oceanic channel has been divided into four smaller basins by introducing a meridional and a zonal strip of land. The width is 1.5° for the latitudinal strip and 2.2° for the longitudinal one. The roughness over land has been set as 0.5 m. The crossed circle denotes an experiment with a halved horizontal eddy diffusion coefficient. The experiments where the SST has been increased (decreased) of 2°C with respect to the initial surface air temperature are denoted with triangles (inverted triangles). The last subset of experiments, denoted with open circles, are

higher-resolution experiments, where a grid step of 0.55° lat and 0.75° long has been used. Three of the experiments adopted specific features. A ''D'' is added to denote a dry cyclone where the precipitation, and the associated release of latent heat, have been suppressed. An ''M'' is added to denote the experiment where the two-way coupling has been restricted to the flux of momentum, while the fluxes of heat and moisture have been computed using Charnock relation. An ''S'' denotes the use of a shorter (28.5°) channel.

The results are summarized in Figs. 11–13. The parameter used is the ratio $\xi = T_w/T_a$, where T_w is an estimate of the time interval during which the wave field is young and T_a is an estimate of the time interval required by the deepening of the cyclone. The value of T_a is defined as the time needed for the low pressure minimum to grow from 50% to 90% of its lowest value. The value of T_w is estimated as $T_w = 3600 \times 125u_{*w}/g$, where u_{*w} is a representative value of the friction velocity. The physical idea behind the above choice is that T_w is proportional to u_{*w}/g. The factor 3600×125 has no influence on the discussion of the results, and it has been chosen in order to give T_w approximately equal to one-half day when $u_{*w} = 1.0$. The representative value u_{*w} has been defined as the average of the maximum friction velocity in a 6-h time interval centered at the instant of the lowest pressure minimum. When the parameter ξ is large, the waves are young during most of the deepening stage of the cyclone so that their effect is expected to be large. Therefore, this parameter can be used to provide a guideline for the interpretation of the results of the simulations.

a. The reduction of the pressure minimum

Figure 11 shows the percentage variation of the pressure minimum $\Delta p/p_c$ as a function of ξ for the experiments listed in Table 1. The amplitude of the pressure variation is $p_c = 1012 - p^{1c}_{\min}$, where 1012 hPa is the pressure unperturbed level and $p^{1c}_{\min}$ is the lowest value of the pressure minimum in the one-way coupled case. The numerator Δp is the average difference in pressure minimum between one-way and two-way experiments in a 6-h interval centered at the time when the low pressure reaches the maximum value. A positive $\Delta p/p_c$ means that the depth of the cyclone is reduced by the two-way coupling. Figure 11 shows that the two-way coupling reduces the depth of the cyclone by an amount that shows a positive trend (in spite of the large scatter) with increasing ξ. The only case that gives $\Delta p/p_c$ negative is an extremely weak cyclone, where the low intensity of the wind implies an old windsea and, consequently, a sea surface roughness lower in the two-way coupled than in the one-way coupled case.

Figure 11 suggests that the effect of the two-way coupling is greater for high-resolution simulations. This is probably due to a more detailed description of the pressure minimum. In fact, the atmospheric evolution turned out to be sensitive to the horizontal resolution in the large amplitude stage of the perturbation, mostly because high resolution increases precipitation and, consequently, latent heat release in the atmosphere, which forces a stronger cyclonic circulation. Although the initial growth rate was similar in the high- and low-resolution cases, the cyclone grew for a longer time in the high-resolution case, reaching much lower pressure at its center and developing, at the same time, more realistic mesoscale structures such as frontal bands and associated low-level jets.

The results of the experiments ''◯wS'' and ''◊m'' reported in Fig. 11 suggest that the two-way coupling effect is larger when a shorter channel is chosen; this is probably due to an increased roughness caused by the action of more rapidly turning winds on the ocean waves. Thus, small-scale storms, such as polar lows, are likely to be more affected by the two-way coupling.

The cases of large SST gradient (denoted by ''s'' and ''e'') reach a lower minimum and are more strongly affected by the two-way coupling than the cases of moderate SST gradient (denoted by ''w'' and ''m''). This indicates that the two-way coupling is more relevant for intense storms. The reason is that intense cyclones that grow in a nearly saturated environment tend to have a rapid evolution and a high surface wind speed, which implies a high value of the parameter ξ. The ''dry'' case, denoted with ''◯sD,'' is intense but is characterized by a much slower evolution so that the parameter ξ is small and the effect of the two-way coupling on the slp minimum is negligible.

b. Reduction of the surface wind speed and significant wave height

The percentage effect on u_{10}, $\Delta u_{10}/u_{10M}$, swh, and $\Delta H_s/H_{sM}$ is shown in Figs. 12 and 13. The variation Δu_{10} is computed by averaging over the same time interval defined above for Δp the difference between the maximum u_{10} in the one-way and two-way coupled experiments. The quantity u_{10M} is the maximum u_{10} in the one-way coupled experiment at the time of the lowest SLP minimum. The analogous definition holds for the significant wave height. The negative values indicate that the quantities are smaller in the two-way coupled experiments. As for the SLP, the effect increases with increasing ξ, reaching a maximum 20% reduction for the swh and 8% for the wind speed.

c. Increase of momentum and heat fluxes

The percentage effect on the friction velocity and total (latent plus sensible) heat fluxes is computed as in sections 5a and 5b.

The effect on the friction velocity is shown in Fig. 14. The resulting values are in the range from 2% to 18%, showing a large scatter but no clear trend with ξ. This is consistent with the analysis carried out in section

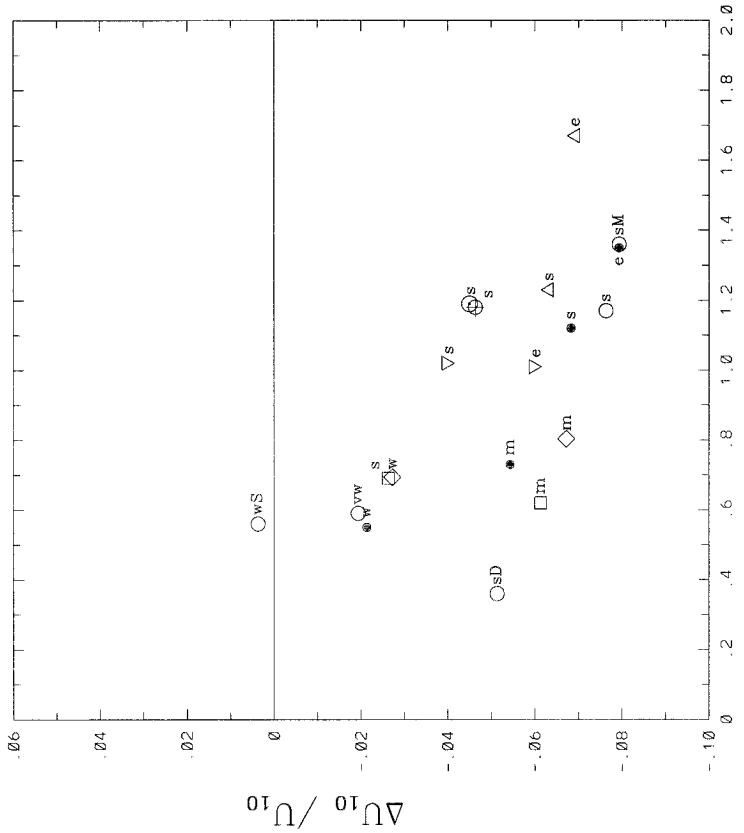

FIG. 12. As in Fig. 11 but for the maximum u_{10}. Negative values mean that the maximum u_{10} is lower in the two-way coupled experiment.

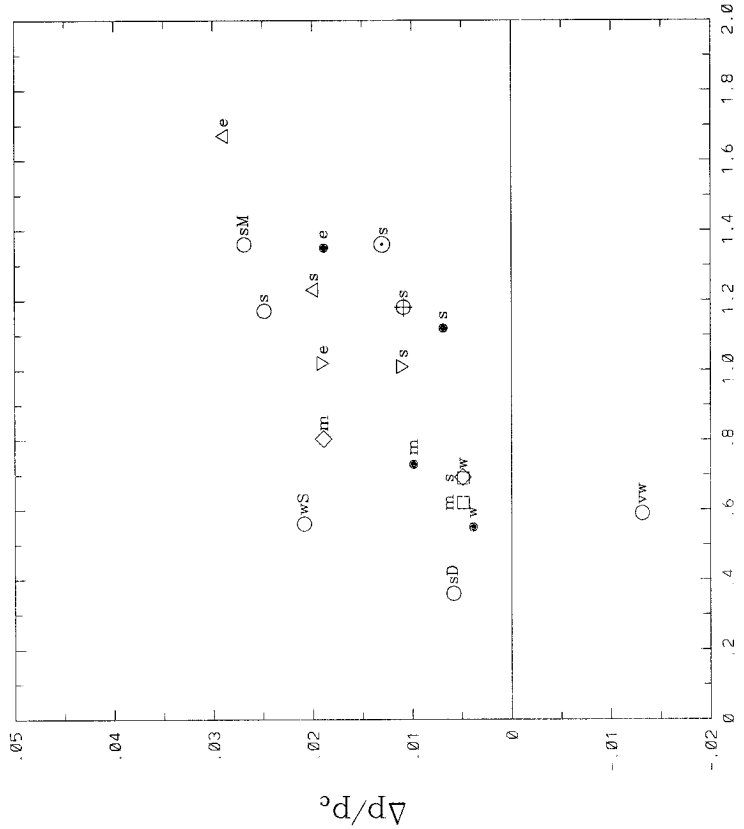

FIG. 11. Percentage variation of the minimum pressure between one-way and two-way coupled experiment for the simulations listed in Table 1 as function of T_w/T_a. Positive values mean that the depth of the pressure minimum is lower in the two-way coupled case. Refer to Table 1 for the meaning of the symbols.

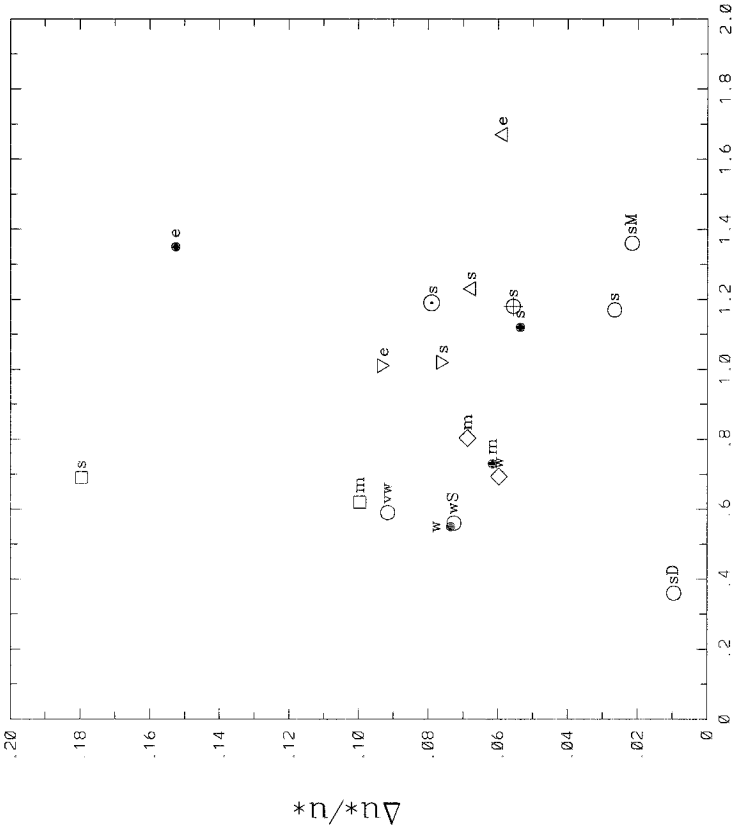

FIG. 14. As in Fig. 11 but for the maximum friction velocity u_*. Positive values mean that the maximum u_* is larger in the two-way coupled experiment.

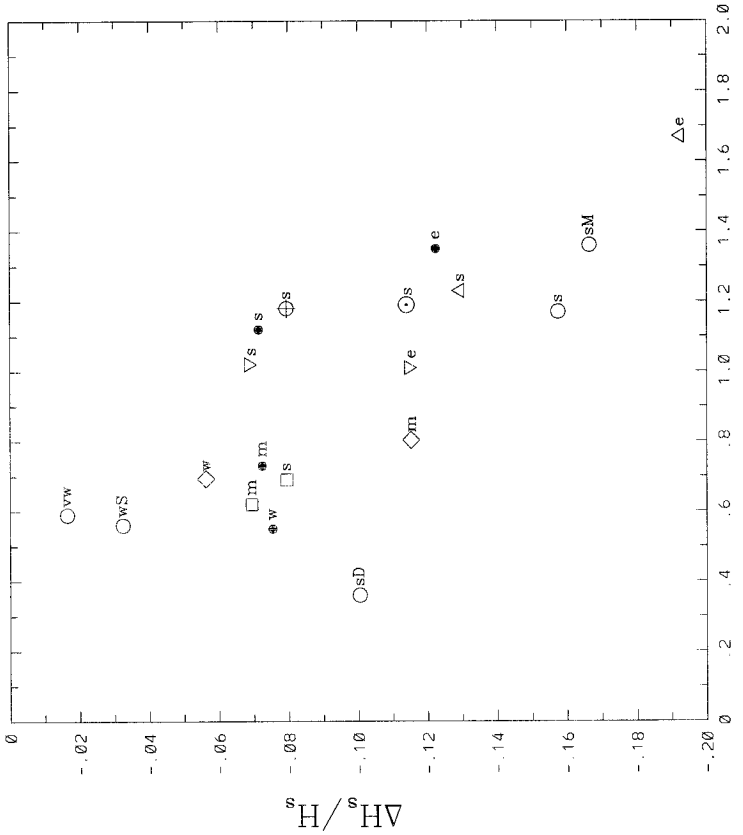

FIG. 13. As in Fig. 11 but for the maximum swh H_s. Negative values mean that the maximum swh is lower in the two-way coupled experiment.

4, where we showed that the maximum value of friction behind the pressure minimum is not greatly modified, while its location is moved to the north in a region of younger windsea. This change of the spatial pattern masks the positive trend with ξ, which remains present in the maximum friction ahead of the cyclone.

The percentage effect on the upward heat flux is shown in Fig. 15. The variation is generally positive, reaching a maximum increase of 20%. Again, the results show a large scatter and no clear trend with ξ. This is presumably because the downward heat flux is placed behind the low pressure minimum, in a region where the effect of the two-way coupling on the sea surface roughness presents a large variability among the experiments carried out in this study. The percentage effect on the downward heat flux is positive and increases with ξ, being larger than 40% in several experiments (Fig. 16). This result is because the downward flux is located ahead of the pressure minimum where the two-way coupling produces sea surface roughness much higher than the one-way coupling.

The ''○sM'' experiment behaves differently, as far as the heat fluxes are concerned, because they are computed using the Charnock relation and the wind speed is reduced because of the wave-dependent roughness. Consequently both upward and downward heat fluxes are reduced, and the variation of heat fluxes are substantially different with respect to the ''○s'' experiment. In spite of this the behavior of ''○s'' and ''○sM'' is similar as far as minimum slp, u_{10}, swh, and friction velocity are concerned. This shows that the variation of the heat flux is not relevant for the development of the cyclone on the short timescale analyzed in this study and that the effect of the two-way coupling on such quantities is only due to the dependence of the momentum flux on the wave field (the importance of the heat flux modification is, presently, a debated question and not supported by any observation or theory).

d. Influence of the coastlines and air–sea temperature difference

The presence of a coastline might be expected to influence the two-way coupling because it reduces the fetch of the wind over sea, decreasing wave age and increasing friction. The experiments ''□m'' and ''□s,'' carried out with two strips of land, as described above, show a very similar behavior. A likely explanation is that the effect of the increased roughness over sea is overwhelmed by the effect of the large roughness present over the nearby land.

If the wave-dependent sea surface roughness is used in the bulk formula for the heat and momentum fluxes at the sea surface, then the effect of two-way coupling could be sensitive to the air–sea stability conditions. However, the results of experiments ''△s'', ''△e'', ''▽s'', and ''▽e'' do not seem to show such an influence. Obviously, an increased SST significantly increases the intensity of the cyclone, while a lower SST slightly decreases it, but this effect is essentially imputable to variations of the (parameterized) atmospheric convective activity, which is quite sensitive to the SST and to the amount of moisture already present in the atmosphere. However, these experiments might be misleading, since the lower troposphere probably reaches a balance with the SST well before the onset of the cyclone.

6. Conclusions

Recent observations and studies consistently indicate an effect of the wave field age on the sea surface roughness, according to which, for a fixed wind speed, roughness is a decreasing function of the wave age. We analyzed how the the evolution of the coupled atmosphere and ocean wave system is affected by the dependence of sea surface roughness on the wave spectrum.

In the storm area, during a fast-growing cyclone, because of the intense and variable wind, the prevalent effects of the two-way coupling are to increase the surface roughness, to enhance the friction velocity, and to reduce the surface wind speed u_{10} and swh. These mechanisms include a negative feedback: on one hand, the friction is increased because a large roughness implies a large drag coefficient; on the other hand, it is decreased because the wind speed of the lowest model level is reduced. The increased friction in the region of intense air–sea interaction is the dominant feature of the two-way coupling that consequently produces a storm with diminished strength. This tendency can be reversed only in a weak, slowly evolving cyclone, where the effect of the two-way coupling resulted a small increase of the low pressure minimum. In the area around the storm, where the wind speed is low and the waves are mainly swell, the sea surface roughness is decreased and the effect of the two-way coupling is a small tendency to decrease the air–sea fluxes.

The effect of the wave field on the two-way coupled atmosphere–wave model has been found to be relevant for the surface fields of u_{10}, u_*, upward and downward heat flux, and swh. The effect on SLP is small (the largest difference is 2.9 Hpa, approximately a 3% reduction of the depth of the pressure minimum), indicating a small effect on the development of the atmospheric low pressure system. In fact, the influence of the two-way coupling on the internal atmospheric variables is discernable only during extreme events and in the central part of the depression. This is because, on the relatively short timescale of these experiments, the development of the cyclone is mostly determined by the initial atmospheric state, while the air–sea fluxes, which are affected by the two way coupling of atmosphere and ocean wave, play a secondary role.

Since the current generation of atmospheric models are capable of simulating the evolution of extratropical cyclones with a reasonable degree of accuracy, only

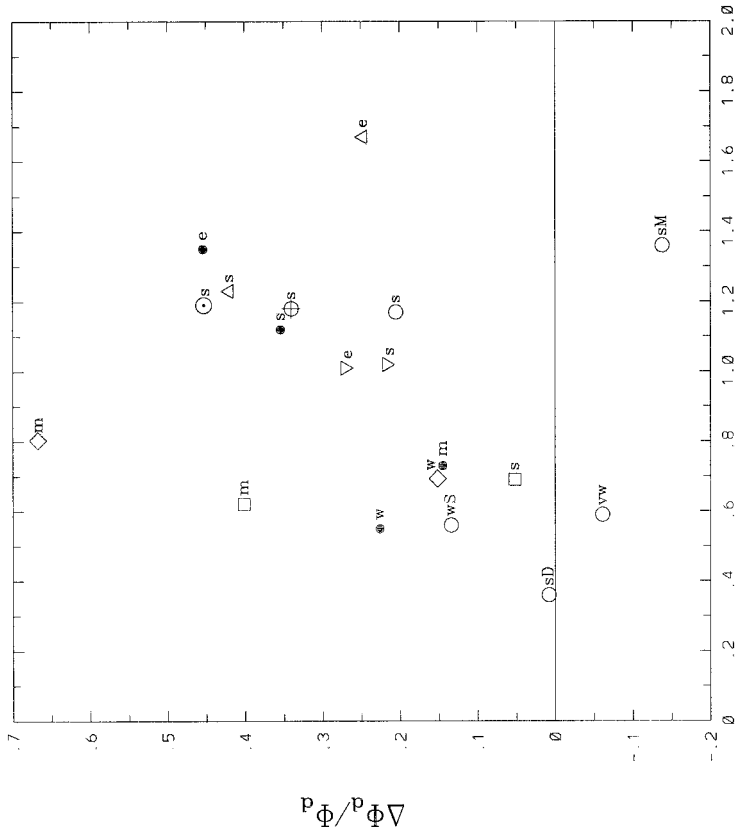

FIG. 16. As in Fig. 11 but for the maximum downward heat flux Φ_d. Positive values mean that the maximum Φ_d is larger in the two-way coupled experiment.

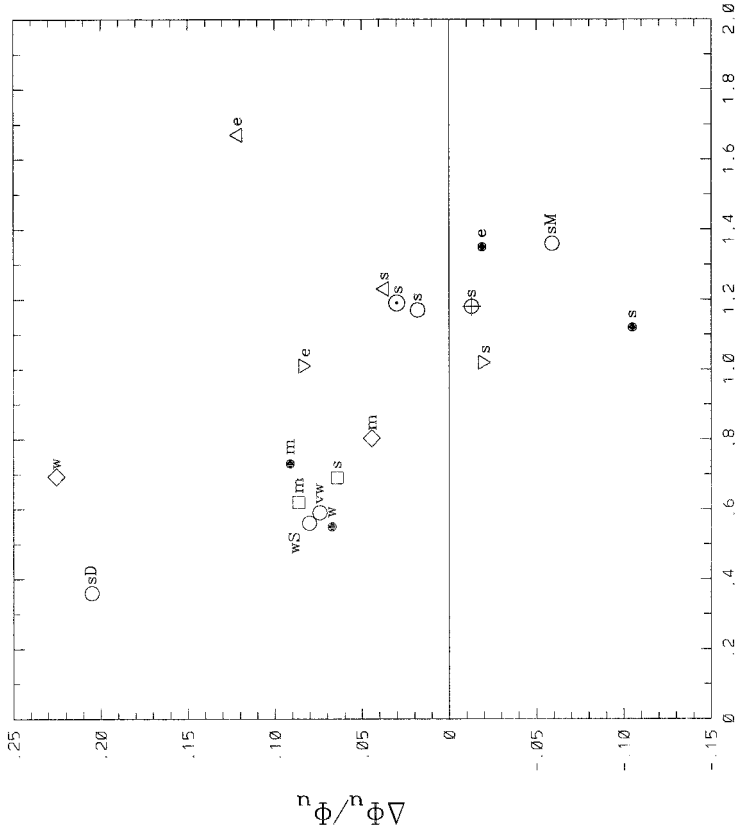

FIG. 15. As in Fig. 11 but for the maximum upward heat flux Φ_u. Positive values mean that the maximum Φ_u is larger in the two-way coupled experiment.

small modifications in SLP have to be expected due to the introduction of coupling with ocean waves. However, systematic errors of magnitude 0.5–3 hPa may have a significant impact in regional forecasting and even more so in climate models. It is therefore interesting to investigate further how the effect of the waves on the atmospheric circulation translates to real cases.

The effect on surface variables is larger and is clearly visible also for weaker cyclones. The increase in the maximum friction velocity and the decrease in the maximum swh are between 10% and 15%, respectively. If proven to be realistic, the increased friction velocity will be relevant for the modeling of storm surges in coastal areas. Moreover, since the effect of the two-way coupling is relevant in the central part of the cyclone where the wind speed and the wave height are large, it might be important for the accurate prediction of such fields and the prevention of loss of life and property.

The large effect on heat fluxes depends on the specification used for the roughness in the computation of the heat transfer coefficient. The heat flux is increased if it is computed using the wave-dependent roughness, while it is decreased if computed using the Charnock relation. In both cases, the effect on the momentum flux remains the same and the attenuation of the cyclone intensity is similar. Consequently, the slightly diminished intensity of the cyclone is mainly due to changes in the momentum transfer coefficient and not to the controversial direct effect of the wave field on heat flux. We conclude that the effect on the atmospheric circulation, albeit small, is probably realistic. Consequently, a future assessment of the direct effect of the wave field on heat transfer appears to be of some importance for the evaluation of the heat flux, but not significant for the computation of SLP, wave field, and momentum flux in coupled atmosphere and ocean wave models.

The behavior of the coupled system has been analyzed using the parameter $\xi = T_w/T_a$, that is, the ratio between the development time of the young windsea T_w and the deepening time of the pressure minimum T_a. A high value of ξ means that the windsea is very young during the deepening of the atmospheric cyclone, and the effect of the wave on the sea surface roughness is large. In fact, the effect of the two-way coupling on the pressure minimum, surface wind speed, swh, and downward heat flux maximum shows an increasing trend with ξ. The parameter ξ is generally large for intense storms because the high friction velocity implies a long development time of the windsea; that is, T_w is large, and they grow rapidly, that is, T_a is short. Therefore, in our experiments the importance of the two-way coupling is conditioned mostly by the intensity of the storm. It is proportionally larger in extreme storms, where the intense and continuously changing wind maintains the waves young for a longer fraction of the storm duration and over a larger area. The effect on the pressure minimum is increased in a high-resolution model, probably because of the more detailed description of the central minimum of the cyclone. Moreover, the effect appears to be larger for cyclones of short wavelength, probably because of the fast turning wind in their central part.

The relation of the two-way coupling to the cyclone intensity explains why no effect of the two-way coupling has been observed in low-resolution climate simulations, where extreme events are rare and not properly reproduced (Weber et al. 1993), in spite of its considerable impact in an extreme single event (Doyle 1994). Our results, though qualitatively similar to those reported by Doyle, do not quantitatively agree with them, in the sense that Doyle's sensitivity of cyclone intensity and surface fluxes to model coupling seems larger than that obtained in the present study. Different model formulation, resolution, and experimental setup do not allow a direct quantitative comparison. Possibly the cyclone simulated by Doyle is more intense than the ones that we simulated, since he adopted a finer grid and a larger SST gradient in the central part of the channel.

It is of practical interest to determine whether an increased Charnock constant can reproduce the increase of sea surface roughness due to young waves, as suggested by simulations of storm surge (Mastenbroek et al. 1993). The same approximation has been tested in this study, repeating the ''extreme'' run with the one-way coupled model and $\alpha_C = 0.032$. This value and the young waves with an age $\alpha_{10} = 0.6$ in two-way coupled models approximately produce the same roughness. The increased Charnock constant simulates the effect of the wave field on the development of the cyclone, but tends to underestimate the changes during the most intense period of the event. On the other hand, the value $\alpha_C = 0.0185$ reproduces very well the average value of the sea surface roughness during the entire development of the storm, while $\alpha_C = 0.032$ produces an overestimation of the sea surface roughness and air–sea fluxes. In this respect, the value $\alpha_C = 0.032$ does not appear to be a generally acceptable approximation because it would produced a biased average roughness with incorrect effect of the resulting climatology of the model.

Finally, we analyzed the average effect of the two-way coupling throughout an intense cyclogenesis event, which is of interest for atmosphere–ocean interaction and climate studies. The reduction in the average swh is significant, but the increase of the average momentum flux is small. The variation of the average heat flux is approximately 10 W m^{-2} and its sign depends on the effect of the wave field on the heat transfer coefficient. If the wave field has a direct influence on the heat transfer coefficient, then the two-way coupling increases the heat flux; otherwise it decreases it.

Note that in this study only the deepening phase of the cyclone has been investigated, and our analysis stops after a first significant minimum value of the low pressure system has been reached. It is likely that during the decay phase, because of the presence of old windsea and a consequently diminished friction, the effect of the two-way coupling will be to slow down the decay of

the cyclone, that is, the two-way coupled case might remain intense for a longer time. Though this study suggests that the effect of the two-way coupling will be a diminished intensity of the storms, the extrapolation of this conclusion to timescales longer than the duration of the marine cyclogenesis cannot be carried out from the material provided by this study.

Obviously this entire investigation represents only a sensitivity study and gives no validation of the expressions used for the transfer coefficients. Since we found that the two-way coupling is of some importance in the computation of the values of swh, wind speed, and air–sea fluxes, its validation by numerical modeling of a realistic situation is possible. The implementation of the coupled model in the Mediterranean Sea, in order to analyze cases of marine cyclogenesis in a complex real situation, is in progress.

Acknowledgments. We are grateful to a reviewer for his careful reading of this paper and for his discussion of our results. The study was supported by the ECA-WOM project of the European Union MAST-II program and by the National Council of Research (CNR) of Italy.

REFERENCES

Banner, M. L., and W. K. Melville, 1976: On the separation of air-flow over waterwaves. *J. Fluid Mech.,* **77,** 825–842.

Buzzi, A., M. Fantini, P. Malguzzi, and F. Nerozzi, 1994: Validation of a limited area model in cases of Mediterranean cyclogenesis: Surface fields and precipitation scores. *Meteor. Atmos. Phys.,* **53,** 137–153.

Charnock, H., 1955: Wind stress on a water surface. *Quart. J. Roy. Meteor. Soc.,* **81,** 639–640.

Donelan, M. A., 1982: The dependence of the aerodynamic drag coefficient on wave parameters. Preprints, *Proc. First Int. Conf. on Meteor. and Air–Sea Interaction of the Coastal Zone,* The Hague, The Netherlands, Amer. Meteor. Soc., 381–387.

——, F. W. Dobson, S. D. Smith, and R. J. Anderson, 1993: On the dependence of sea surface roughness on wave development. *J. Phys. Oceanogr.,* **23,** 2143–2149

Doyle, J. D., 1994: Air–sea interaction during marine cyclogenesis. *The Life Cycles of Extratropical Cyclones,* Vol. III, University of Bergen, 61–66.

Emanuel, K., M. Fantini, and A. J. Thorpe, 1987: Baroclinic instability in an environment of small stability to slantwise moist convection. Part I: Two-dimensional models. *J. Atmos. Sci,* **44,** 1559–1573.

Geernaert, G. L., S. E. Larsen, and F. Hansen, 1987: Measurements of the wind stress, heat flux, and turbulence intensity during storm conditions over the North Sea. *J. Geophys. Res.,* **92,** 13 127–13 139.

Hasselmann, K, and T. P. Barnett, E. Bouws, H. Carlson, D. E. Cartwright, K. Enke, J. A. Ewing, H. Gienapp, D. E. Hasselmann, P. Krusemann, A. Meerburg, P. Muller, D. J. Olbers, K. Richter, W. Sell, and H. Walten, 1973: Measurements of wind-wave growth and swell decay during the Joint North Sea Wave Project (JONSWAP). *Dtsch. Hydrogr. Z.,* (Suppl. A), **8,** 22 pp.

——, H. Günther, and P. A. E. M. Janssen, 1993: The WAM Model Cycle 4. DKRZ Rep. No. 14, 91 pp. [Available from Max Planck Institut für Meteorologie, Bundesstrasse 55, D-20146, Hamburg, Germany.]

Janssen, P. A. E. M., 1989: Wave induced stress and the drag of the air flow over sea waves. *J. Phys. Oceanogr.,* **19,** 745–754.

——, 1991: The quasi-linear theory of wind wave generation applied to wave forecasting. *J. Phys. Oceanogr.,* **21,** 1631–1642.

——, P. Lionello, and L. Zambresky, 1989: On the interaction of wind and waves. *Philos. Trans. Roy. Soc. London* **329A,** 289–301.

Kitaigorodsky, S. A., 1973: *The Physics of Air–Sea Interaction.* Israel Program for Scientific Translation, 237 pp.

Lionello, P., K. Hasselmann, and G. L. Mellor, 1993: On the coupling between an ocean wave model and a model of the mixed layer. *Proc. of the Air–Sea Interface Symp.,* Marseille, France, University of Miami, 195–201.

Louis, J. F., M. Tiedtke, and J. F. Geleyn, 1981: A short history of operational PBL parameterization at ECMWF. *Workshop on PBL Parameterization,* Reading, United Kingdom, ECMWF, 59–79.

Makin, V. K., V. N. Kudryavtsev, and C. Mastenbroek, 1995: Drag of the sea surface. *Bound.-Layer Meteor.,* **73,** 159–182.

Mastenbroek, C., C. J. Bergers, and P. A. E. M. Janssen, 1993: The dynamical coupling of a wave model and a storm surge model through the atmospheric boundary layer. *J. Phys. Oceanogr.,* **23,** 1856–1866.

Melville, W. K., 1977: Wind stress and roughness length over breaking waves. *J. Phys. Oceanogr.,* **7,** 702–710.

Smith, S. D., and Coauthors, 1992: Sea surface wind stress and drag coefficients: The HEXOS results. *Bound.-Layer Meteor.,* **60,** 109–142

Toba, Y., N. Lida, H. Kawamura, N. Ebuchi, and I. S. F. Jones, 1990: Wave dependence of sea-surface wind stress. *J. Phys. Oceanogr.,* **20,** 705–721.

The WAMDI group (S. Hasselmann, K. Hasselmann, E. Bauer, P. A. E. M. Janssen, G. Komen, L. Bertotti, P. Lionello, A. Guillaume, V. C. Cardone, J. A. Greenwood, M. Reistad, L. Zambresky, and J. A. Ewing), 1988: The WAM model—A third generation ocean wave prediction model. *J. Phys. Oceanogr.,* **18,** 1776–1810.

Weber, S. L., H. von Storch, P. Viterbo, and L. Zambresky, 1993: Coupling an ocean-wave model to an atmospheric general circulation model. *Climate Dyn.,* **8,** 63–69.

Wu, J. 1982: Wind-stress coefficient over sea surface from breeze to hurricane. *J. Geophys. Res.,* **87,** 9704–9706.